Chem Soc Rev

Recent progress in tailored growth of two-dimensional hexagonal boron nitride via chemical vapour deposition

Journal:	*Chemical Society Reviews*
Manuscript ID	CS-TRV-02-2018-000167.R1
Article Type:	Tutorial Review
Date Submitted by the Author:	01-Apr-2018

Complete List of Authors:	Sun, Jingyu; Soochow Institute for Energy and Materials InnovationS (SIEMIS), Key Laboratory of Advanced Carbon Materials and Wearable Energy Technologies of Jiangsu Province, Soochow University Chen, Lu; Soochow University Song, Yingze; Soochow University Ji, Qingqing; Massachusetts Institute of Technology Song, Xiuju; Rutgers University Li, Qiucheng; Soochow Institute for Energy and Materials InnovationS (SIEMIS), Key Laboratory of Advanced Carbon Materials and Wearable Energy Technologies of Jiangsu Province, Soochow University Zhang, Yanfeng; Peking University, Center for Nanochemistry (CNC), Beijing National Laboratory for Molecular Sciences, State Key Laboratory for Structural Chemistry of Unstable and Stable Species, College of Chemistry and Molecular Engineering, Academy for Advanced Interdisciplinary Studies Zhang, Li; Soochow University, School of Energy Kong, Jing; MIT (Engineering), Department of Electrical Engineering and Computer Science Liu, Zhongfan; Peking University, College of Chemistry and Molecular Engineering

Journal Name

ARTICLE

Recent progress in tailored growth of two-dimensional hexagonal boron nitride *via* chemical vapour deposition

Received 00th January 20xx,
Accepted 00th January 20xx

DOI: 10.1039/x0xx00000x

www.rsc.org/

Jingyu Sun*[a], Chen Lu[a], Yingze Song[a], Qingqing Ji[b], Xiuju Song[c], Qiucheng Li[a], Yanfeng Zhang[d], Li Zhang*[a], Jing Kong[b] and Zhongfan Liu*[ad]

Recent years have witnessed many advances in two-dimensional (2D) hexagonal boron nitride (h-BN) materials in both fundamental research and practical applications. This has ultimately been inspired by the unique electrical and optical properties, as well as the excellent thermal and chemical stability of h-BN. However, controllable and scalable preparation of 2D h-BN materials has been challenging. Very recently, the chemical vapour deposition (CVD) technique has shown great promise to attain high-quality h-BN samples with excellent layer-number selectivity and large-area uniformity, considerably contributing to the latest advancements of 2D material research. In this tutorial review, we provide a systematic summary of the state-of-the-art in the tailored production of 2D h-BN on various substrates by virtue of CVD routes.

Key learning points
(1) Detailed case-studying for the CVD growth of 2D h-BN on various substrates
(2) Highlight of recent advances in the CVD synthesis of 2D h-BN
(3) Characterization of the crystal quality of as-grown h-BN on metals and dielectrics
(4) Summary of latest explorations in employing h-BN as a 2D growth substrate
(5) The practical device applications of CVD-derived h-BN materials

1. Introduction

Inspired by the 'graphene gold rush', two-dimensional (2D) atomic crystals (beyond graphene) have nowadays been attracting an ever-growing attention in diverse fields and applications.[1,2] The beauty of these novel materials lies in the fact that such 2D sheets afford strictly defined dimensionalities desired in a plethora of essential material categories, encompassing conductors, semiconductors, and insulators.[3] As a typical graphene analogue material, 2D hexagonal boron nitride (h-BN), an insulator with a direct band gap (5.9 eV), has stimulated intense research interest owing to their appealing properties such as good oxidation resistance up to 850 °C, excellent chemical stability to acid, high thermal conductivity, superior elastic modulus, and good mechanical flexibility.[4] More significantly, h-BN has been identified as a promising candidate as a dielectric layer or protecting encapsulator for 2D electronic devices, because of its atomically flat surface without dangling bonds and charged impurities. In this regard, ultrahigh carrier mobility (~60000 $cm^2 \cdot V^{-1} \cdot s^{-1}$ at room temperature) was demonstrated in graphene transistors employing h-BN as a substrate,[5] and a ballistic transport over 28 μm was observed in graphene sandwiched between few-layer h-BN flakes.[6] The exceptional insulating and thermal-conducting nature of h-BN also ensures its practical uses as a key building-block in light-weight, high-performance wearable and flexible electronic systems.[3,7]

The continuous exploration of fascinating properties of h-BN and the urgent request in building up miniaturized functional devices have driven the relevant research fields to rapidly develop. One major and important field of h-BN is the reliable preparation of layer-controllable, high-quality crystals and films at a large scale. To date, two main strategies have been developed to realize h-BN production: One is the top-down exfoliation from bulk h-BN crystals with the aid of mechanical forces; the other is the bottom-up growth route by virtue of chemical vapour deposition (CVD) technique. The top-down exfoliation would give rise to high-quality h-BN crystals, but with limited yields and small lateral sizes (up to several microns). As such, h-BN flakes produced by the dry, mechanical cleavage are often used for designing and fabricating proof-of-concept devices. The liquid-phase exfoliation would indeed enable the generation of well-

[a] Soochow Institute for Energy and Materials InnovationS (SIEMIS), Key Laboratory of Advanced Carbon Materials and Wearable Energy Technologies of Jiangsu Province, Soochow University, Suzhou, Jiangsu 215006, P. R. China. E-mail: sunjy86@suda.edu.cn; zhangli81@suda.edu.cn
[b] Department of Electrical Engineering and Computer Science, Massachusetts Institute of Technology, Cambridge, Massachusetts 02139, USA.
[c] Department of Materials Science & Engineering, Rutgers University, Piscataway, New Jersey 08854, USA.
[d] Center for Nanochemistry (CNC), College of Chemistry and Molecular Engineering, Peking University, Beijing 100871, P. R. China. E-mail: zfliu@pku.edu.cn

dispersed 2D h-BN nanosheets from their bulk counterparts at a large quantity. It also gains control over flake thickness, but suffering from a quite wider thickness distribution. In addition, such wet exfoliation route still limit the lateral sizes of 2D crystals (*e.g.*, normally < 100 μm), as well as might introduce extrinsic contaminations that jeopardize the quality and properties of resultant h-BN flakes.[4]

Recent years have witnessed a growing interest in the bottom-up synthesis of h-BN crystals and films by means of CVD. Being a scalable and reliable technique, the CVD method has shown great promise to attain large-area h-BN samples with excellent layer-number selectivity and controllable quality, which has considerably contributed to the latest advancements of 2D material research. A unique characteristic of the CVD route lies in the fact that it allows to delicately tailor the morphologies and properties of as-synthesized h-BN by adjusting synthetic parameters such as the growth temperature, the type of BN precursors, the process pressure, and the carrier gas ratio. For the time being, such a method is likely the most successful and versatile route for achieving wafer-scale, high-quality h-BN films in a relatively simple and economic fashion.

In this tutorial review, the recent advances in the field of CVD growth of h-BN will be extensively summarized. We will first introduce the typical strategies for the deposition of 2D h-BN materials, splitting by two representative routes of thermal CVD and plasma-enhanced CVD (PECVD). We follow with a detailed presentation on the controlled growth of h-BN on various substrates by case-studying different metals as well as dielectrics. We will also discuss the growth of 2D vertical heterostructures using CVD-derived h-BN as a growth substrate. Following the brief introduction of device applications of h-BN materials, we conclude in the last section with an overview of the challenges and perspectives on the tailored synthesis of h-BN *via* CVD. A timeline detailing the main milestones is illustrated in **Fig. 1**, which reveals the history of the development of CVD preparation of h-BN on various substrates.[9-24] In the past several years, there have, indeed, been significant improvements in the CVD synthesis of h-BN; however, to the best of our knowledge, a lack of comprehensive review articles dealing with controlled production of h-BN by means of CVD techniques. A latest exciting review by Cai *et al.* highlighted recent developments in the controlled CVD growth of 2D crystals, but with an emphasis on semiconducting transition metal dichalcogenides (TMDs).[7] The review we present here aims for readers who are interested in this emerging field of 2D material research.

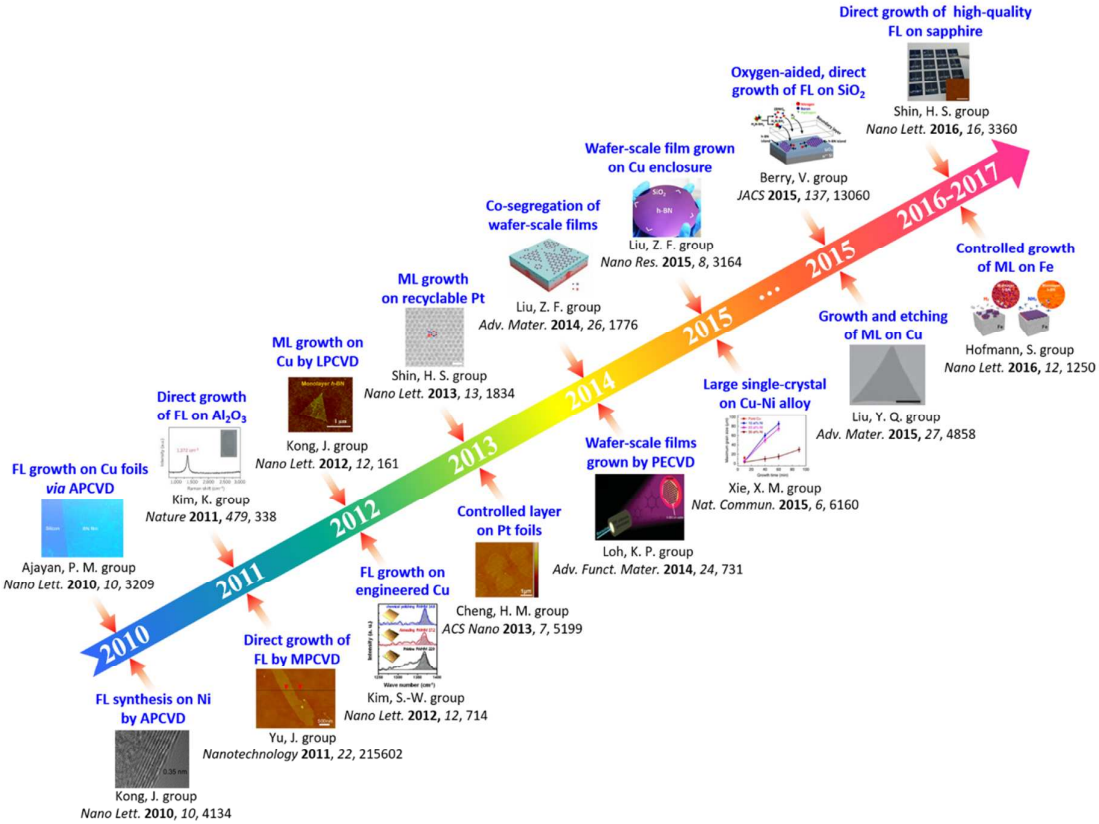

Fig. 1 A brief chronology of the key development of tailored growth of 2D h-BN *via* CVD. Abbreviation: FL-few layer; ML-monolayer; APCVD-atmospheric pressure CVD; LPCVD-low pressure CVD; MPCVD-microwave plasma CVD; PECVD-plasma-enhanced CVD. Images reproduced with permission as follows: "FL growth on Cu foils *via* APCVD": reproduced with permission from ref. 9. Copyright 2010, American Chemical Society. "FL synthesis on Ni by APCVD": reproduced with permission from ref. 10. Copyright 2010, American Chemical Society. "Direct growth of FL on Al_2O_3": reproduced with permission from ref. 11. Copyright 2011, Nature Publishing Group. "Direct growth of FL by MPCVD": reproduced with permission from ref. 12. Copyright 2011, IOP Publishing. "ML growth on Cu by LPCVD": reproduced with permission from ref. 13. Copyright 2012, American Chemical Society. "FL

growth on engineered Cu": reproduced with permission from ref. 14. Copyright 2012, American Chemical Society. "ML growth on recyclable Pt": reproduced with permission from ref. 15. Copyright 2013, American Chemical Society. "Controlled layer on Pt foils": reproduced with permission from ref. 16. Copyright 2013, American Chemical Society. "Co-segregation of wafer-scale films": reproduced with permission from ref. 17. Copyright 2014, Wiley-VCH. "Wafer-scale films grown by PECVD": reproduced with permission from ref. 18. Copyright 2014, Wiley-VCH. "Wafer-scale film grown on Cu enclosure": reproduced with permission from ref. 19. Copyright 2015, Springer International Publishing AG. "Large single-crystal on Cu-Ni alloy": reproduced with permission from ref. 20. Copyright 2015, Nature Publishing Group. "Oxygen-aided, direct growth of FL on SiO_2": reproduced with permission from ref. 21. Copyright 2015, American Chemical Society. "Growth and etching of ML on Cu": reproduced with permission from ref. 22. Copyright 2015, Wiley-VCH. "Direct growth of high-quality FL on sapphire": reproduced with permission from ref. 23. Copyright 2016, American Chemical Society. "Controlled growth of ML on Fe": reproduced with permission from ref. 24. Copyright 2016, American Chemical Society.

2. Typical routes for the CVD growth of h-BN

The tailored preparation of 2D materials with high-quality, large-scale uniformity and layer controllability accounts for an ultimate pursuit for real applications in electronic and optical devices. In recent years, CVD technique has been considered as an emerging paradigm to realize this goal, especially for the case of graphene. The development of CVD graphene growth methodologies has in turn stimulated researchers to apply the similar approaches within the scope of 2D h-BN production. The obtained h-BN flakes or films *via* rationally-designed CVD processes could be used as insulating/protecting layers that rival ubiquitous SiO_2 in nanoelectronics and/or as growth substrates for building-up 2D heterostructures. Nowadays the CVD synthesis of 2D h-BN on various substrates (including metals and insulators) has been proven to be readily practicable, offering new opportunities for device fabrication and applications.

It is worth-mentioning that considerable attempts were focused on cubic-BN (c-BN) synthesis at the initial stage of BN growth studies, where Takahashi's work employing BCl_3 precursor was amongst the pioneer researches on growing BN *via* CVD.[8] Over the past few years huge efforts have been devoted to the controlled deposition of 2D h-BN on substrates. Herein, we do not focus on the work carried out under ultrahigh vacuum conditions, which were already well summarized in previous review article by Pakdel *et al.*[4] In contrast, due to the lack of an exhaustive analysis of the progression of in-practical CVD routes, we report here a detailed summary of the most prominent research papers published from the year of 2010 onwards regarding the tailored preparation of 2D h-BN with large scalability on suitable substrates aiming for practical applications. In this sense, a number of deposition techniques have been employed and such techniques can be classified into two main methodologies, namely, thermal CVD and PECVD.

The thermal CVD involves the thermal activation of BN precursors and the subsequent chemical reaction leading to the formation of 2D h-BN flakes or films over a desired substrate. The energy demanded within the whole process is supplied by heat. As shown in **Fig. 2a**, the set-up for a thermal CVD process to grow h-BN is quite straightforward: a piece of substrate is loaded in a quartz-tube heating chamber, which is connected with a BN precursor supplier at its upstream as well as a vacuum pump at its downstream. The chamber is heated to the designed growth temperature prior to the introduction of the BN precursor, such as ammonia borane. The chamber pressure can be delicately set by controlling the pumping rate, enabling the growth at a relatively low pressure (LPCVD), or at atmospheric pressure (denoted as APCVD). The choice over LPCVD and APCVD depends heavily upon the availability of instruments and the aimed product. The differentiation in the operating pressure is key to determining whether the CVD reaction is mass transport controlled (APCVD) or surface reaction rate controlled (LPCVD). In this fashion, the size of the obtained h-BN films is only limited by the employed substrate. The BN precursor can be supplied by a gaseous mixture (diborane and ammonia), a liquid-phase compound (borazine), or a solid-state substance (ammonia borane).

On the other hand, in a PECVD system the activation and dissociation of BN precursor is effectively carried out with the aid of plasma, which is normally generated by microwave discharge or radio frequency (RF) techniques (**Fig. 2b**). The plasma can provide a highly reactive chemical environment that could lower the process temperature and improve the growth rate of h-BN as compared to that of a thermal CVD. Therefore the PECVD process enables an efficient growth of 2D h-BN material at relatively lower growth temperature (*i.e.*, < 850°C). For instance, continuous, few-layer films can be obtained at 800°C with a short deposition time of 3 min, as reported by Zhang *et al.*[18]

A further distinction of CVD route could be in relation to the CVD reactor on whether it is a hot-wall or a cold-wall. As for a hot-wall CVD, gas precursors tend to react in hot zone prior to reaching the substrate, and hence the gas atmosphere unpredictably varies along the flow direction. Revolutionary growth methods are nowadays being developed with respect to the localized injection of gas precursors precisely down to the desired places of the growth substrate in a controllable manner.

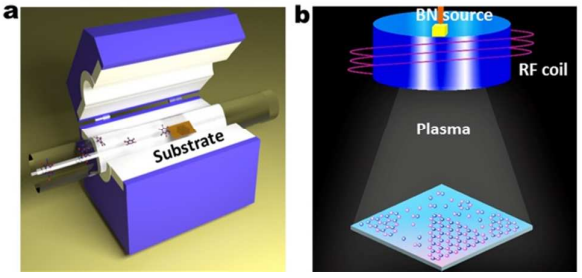

Fig. 2 Schematic illustration of the 2D h-BN growth process using (a) thermal-CVD and (b) PECVD route.

3. Controllable growth of h-BN on metals

As the 2D h-BN synthesis on metals *via* CVD is a heterogeneous catalytic chemical reaction process, the metal plays significantly dual roles to serve as the substrate and catalyst. In recent years, key efforts have been paid to synthesize high-quality 2D h-BN on metals. Herein the term "high-quality" denotes that the as-produced h-BN possesses key advantages including high crystallinity, low defect density and large crystal sizes. The quality of h-BN could be evaluated by means of various characterisation tools, such as scanning electron microscopy (SEM; for crystal size inspection), atomic force microscopy (AFM; for layer number identification), X-ray photoelectron spectroscopy (XPS; for stoichiometry evaluation) and electron diffraction technique (for single crystal identification). In particular, the defect density of h-BN crystals could be exclusively probed by ultra-high vacuum scanning tunnelling microscopy (UHV-STM) and high-resolution transmission electron microscopy (HR-TEM). In this section, we review the latest advances in details by case-studying the controlled growth on catalytically-active, widely-used metallic substrates, including Cu, Pt, Ni, Fe and metal alloys.

3.1 Copper

3.1.1 Layer number control. Controlling the layer number of h-BN with large-scale uniformity is of great significance, for example, few-layer h-BN film is desirable as a promising dielectric for electronic devices. There have been intensive research attempts to produce h-BN with good layer number control, especially on Cu. Pioneer work by Song *et al.* demonstrated large-area synthesis of h-BN film (2-5 layers) using an APCVD system with ammonia borane serving as the precursor.[9] As-grown film displays reasonable quality as confirmed by the optical microscope (OM) image (**Fig. 3a**), SEM and TEM characterisations (**Fig. 3b** and **Fig. 3a** inset). Similar APCVD growth of h-BN was also carried out on engineered Cu foils by Lee *et al.*, where the surface morphology control of Cu by increasing its grain size and improving its surface flatness was crucial for obtaining high-quality, few-layer h-BN.[14] On the other hand, the precise layer number control down to a monolayer requires more delicate manipulation over the synthetic parameters, in particular the chamber pressure. Kim *et al.*'s work is among the earliest studies on synthesizing monolayer 2D h-BN on Cu.[13] The growth was performed by LPCVD employing a two-heating-zone set-up. Clean monolayer h-BN triangular flake (**Fig. 3c**) as well as complete monolayer film (**Fig. 3d** and inset) can be grown under such a LPCVD condition. It was suggested that an LPCVD process was advantageous in realizing monolayer preparation since the growth was preferentially surface-mediated and less affected by the gas-flow effect.

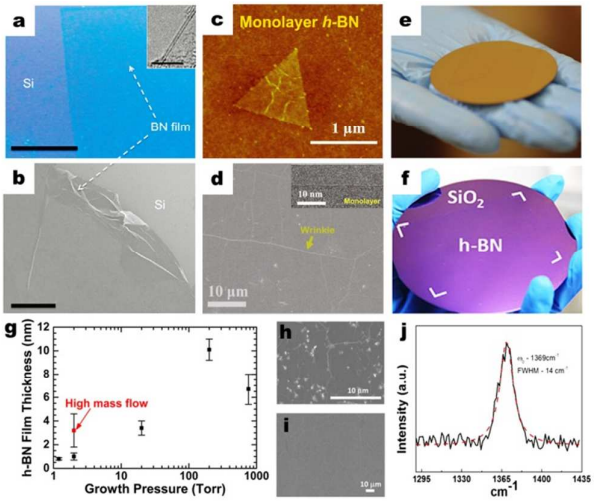

Fig. 3 Layer number control of h-BN grown on Cu. (a) OM image showing a large-area h-BN film. Scale bar, 1 cm. (b) SEM characterisation of as-grown film transferred onto Si substrate. Scale bar, 10 μm. Inset: HRTEM image of film edge showing its few-layer thickness. Reproduced with permission from ref. 9. Copyright 2010, American Chemical Society. (c) AFM image of a monolayer h-BN triangle. (d) SEM image of a continuous monolayer h-BN. Inset: HRTEM image showing the h-BN film are indeed monolayer. Reproduced with permission from ref. 13. Copyright 2012, American Chemical Society. (e) Photograph showing a 2-inch wafer-sized, few-layer h-BN film. Reproduced with permission from ref. 18. Copyright 2014, Wiley-VCH. (f) Photograph of a 4-inch wafer scale, uniform monolayer h-BN film. Reproduced with permission from ref. 19. Copyright 2015, Springer International Publishing AG. (g) h-BN film thickness *vs.* growth pressure, suggesting the production of thin h-BN films at LPCVD. Reproduced with permission from ref. 25. Copyright 2016, American Chemical Society. (h) SEM image of thicker h-BN film generated under fast heating of precursor. (i) SEM image of clean film with monolayer thickness under a slow heating. (j) Raman spectrum of h-BN monolayer. Reproduced with permission from ref. 26. Copyright 2015, American Chemical Society.

Producing high-quality h-BN film with perfect large-area uniformity is technologically intriguing for practical applications. In this sense, Zhang *et al.* succeeded in the preparation of 2-inch wafer-sized, few-layer h-BN films on $Cu/SiO_2/Si$ substrate using borazine *via* a PECVD route (**Fig. 3e**).[18] The homogeneous h-BN film at a wafer scale guaranteed its use as a large-area dielectric layer for graphene plasmonics. Moreover, predominantly monolayer h-BN film was demonstrated by Song *et al.* at a 4-inch-wafer scale (**Fig. 3f**), where AFM height measurements confirmed that the entire sample consisted of ~92% monolayer.[19]

Indeed, dictating the layer number of h-BN films during the CVD process is non-trivial as it demands fine control over the growth protocols. Recently, a systematic investigation by Koepke *et al.* examined the role of pressure in the CVD growth of h-BN films from ammonia borane.[25] It was found that the h-BN growth was pressure-sensitive where synthesis by LPCVD gave rise to a thin and planar product (**Fig. 3g**). This could be attributed to the fact that LPCVD conditions increased the mass transport coefficient h_g, promoting surface catalysis (h_g » K_s; K_s: surface growth rate) and accordingly producing uniform sp^2 h-BN. Another study by Stehle and co-workers revealed that variation of precursor dosage (ammonia borane) during an APCVD reaction exerted a clear impact on the layer number

as well as quality of resultant h-BN films.[26] In this regard, slow and controlled heating of precursor resulted in a complete monolayer film without apparent multilayers (**Fig. 3h-j**).

3.1.2 Domain size enlargement. There have been relentless efforts in synthesizing 2D h-BN crystals with enlarged domain sizes. However, it seems difficult to obtain similar-sized h-BN flakes on Cu as the case of graphene single crystals, which can be of centimetre-scale. This might be due to the greater chemical affinity of N-containing intermediates to the Cu surface than that of carbon intermediates.[19] In this sense, enlarging the domain size of h-BN on Cu requires effective treatment of the substrate and/or special design of growth protocols, mainly in order to suppress the nucleation density of h-BN.

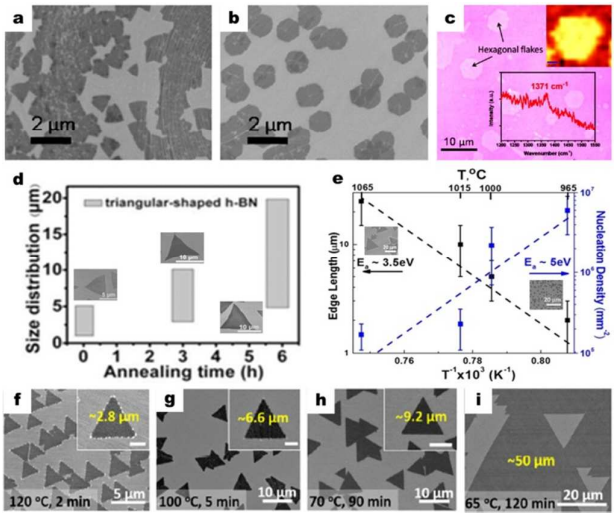

Fig. 4 Domain size enlargement of h-BN flakes grown on Cu. (a) SEM image of triangular h-BN domains grown on unpolished Cu. (b) SEM image of hexagonal-shaped h-BN domains grown on polished Cu. (c) OM micrograph of h-BN hexagons on SiO_2/Si substrate. Inset showing a corresponding Raman spectrum and a Raman mapping image. Reproduced with permission from ref. 27. Copyright 2014, American Chemical Society. (d) Size distributions of h-BN domains as a function of annealing time for Cu foils. Reproduced with permission from ref. 22. Copyright 2014, Wiley-VCH. (e) Arrhenius plot showing the average edge length and the nucleation density *vs.* growth temperature. Reproduced with permission from ref. 26. Copyright 2015, American Chemical Society. (f-i) SEM images of the size evolution of h-BN triangles grown at different precursor heating temperatures and growth times. Reproduced with permission from ref. 19. Copyright 2015, Springer International Publishing AG.

Improving the surface flatness of Cu substrates represented a straightforward and efficient way to reduce the nucleation density of h-BN while increase the domain sizes. In 2014, Tay *et al.* realized the growth of relatively large hexagonal-shape h-BN domains (~35 μm^2) by electropolishing the employed Cu foils (**Fig. 4a-c**).[27] Wang *et al.* demonstrated that prolonged pre-annealing of Cu substrate up to 6 h led to obtaining large-sized h-BN flakes (~170 μm^2), which was 4-5 times larger than that achieved in previous studies (**Fig. 4d**).[22]

Stehle *et al.* found that the size of h-BN crystals was of strong temperature-dependence during an APCVD process, where higher temperature boosted the growth of larger-sized flakes, reaching ~170 μm^2 in size in 30 min under 1065°C (**Fig. 4e**).[26] Intentionally, Song *et al.* employed a folded Cu enclosure to grow h-BN flakes on its inner surface.[19] Systematic tuning the precursor feeding rate enabled the fine control over the nucleation density towards the realization of large-area flakes (**Fig. 4f-i**). In this case, the size of as-prepared single-crystalline triangular domain was as large as ~2200 μm^2 (up to ~72 μm in edge length).[19]

3.1.3 Domain shape engineering. h-BN contains two different elements, boron and nitrogen, and hence possesses greater variation in domain's termination patterns. Nitrogen termination is in general considered to be energetically favourable as compared to the boron termination, *e.g.*, the commonly-grown triangular flake on Cu is nitrogen-terminated. h-BN can also take other shapes such as truncated triangles and hexagons with their edges having both nitrogen- and boron-terminations.

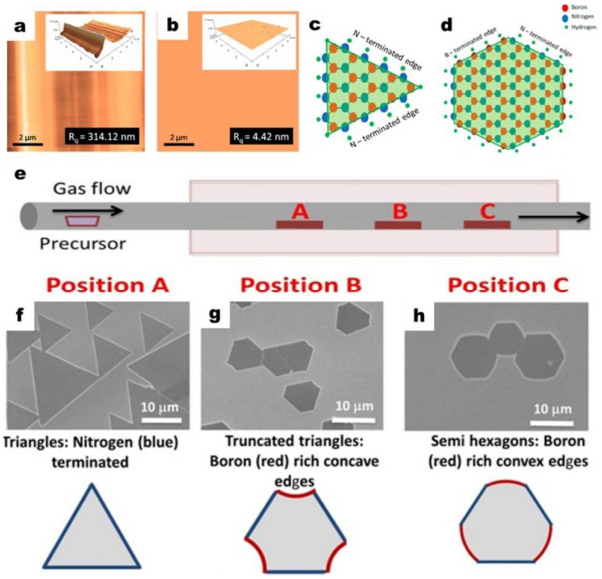

Fig. 5 Domain shape engineering of h-BN flakes grown on Cu. (a and b) AFM images with corresponding surface roughness value, 314.12 and 4.42 nm of (a) unpolished and (b) polished Cu foils, respectively. (c and d) Illustration of atoms arrangement on a monolayer triangular and hexagonal-shape h-BN domains. Reproduced with permission from ref. 27. Copyright 2014, American Chemical Society. (e) APCVD experimental setup for h-BN growth with Cu substrates placed at the position A, B and C. (f-h) SEM images of the h-BN domains grown at 1065 °C using argon as a carrier gas, with the schematic illustration of as-grown h-BN crystal shapes and corresponding terminations. Reproduced with permission from ref. 26. Copyright 2015, American Chemical Society.

Shape control of h-BN domains could be achieved by the treatment of Cu substrate, *i.e.* the creation of an oxygen-abundant surface, as exemplified by the growth on electropolished Cu foils.[27] The high surface oxygen contents played a key role in the reduction of edge-attachment energy barrier; in turn, the active BN species had sufficient energy to bond onto both nitrogen- and boron-terminated edges, thereby forming hexagonal-shaped domains (**Fig. 5a-d**).

Recent theoretical work led by Yakobson and colleagues revealed that shape variation of h-BN domains can be manipulated by adjusting the chemical balance between boron and nitrogen (*i.e.*, the ratio of boron to nitrogen active species concentrations on the copper surface).[28] This can be simply

realized by deliberate positioning of Cu substrate during an APCVD reaction (**Fig. 5e**).[26] A clear shape evolution from triangle to hexagon was observed as the substrate position moved away from the precursor inlet (with pure argon serving as the carrier gas), and was associated with the deficiency of activated nitrogen-containing species closer to the CVD tube outlet (**Fig. 5f-h**).[26]

3.1.4 Domain orientation tailoring. The synthesis of 2D h-BN with controlled orientation is a prerequisite for the complete formation of a large-area, single-crystalline film. Extensive exploration in the growth of h-BN on Cu showed that the separated h-BN domain orientations were notably correlated with respect to the underlying substrate orientations. In this regard, Song *et al.* conducted a rigorous analysis of the as-grown h-BN domain orientations on Cu foils with the aid of SEM, electron backscatter diffraction (EBSD) mapping and density functional theory (DFT) calculations.[19] Upon annealing the Cu enclosure in a LPCVD process, three dominant facets, namely Cu (111), Cu (100) and Cu (110) could be easily obtained. It can be seen from **Fig. 6** that different Cu facets yield distinctly predefined h-BN orientations, within which the h-BN triangles are well aligned on the Cu (111) facet. Further DFT calculation results were in good agreement with the experimental observations, suggesting that the uniformly-orientated domains on Cu (111) can be interpreted as the energetically preferred orientations of the h-BN. Such an excellent alignment of h-BN domain over the Cu (111) surface opens up a potential way to realize single-crystalline h-BN film at a large area.

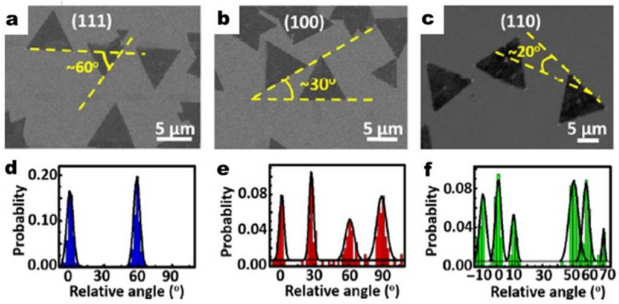

Fig. 6 Domain orientation tailoring of h-BN flakes grown on Cu. (a-c) Representative SEM images of h-BN domains grown on Cu (111), Cu (100) and Cu (110), respectively. (d-f) Corresponding statistical distributions of the edge angles of individual triangular h-BN domains grown on Cu (111), Cu (100) and Cu (110) faces, respectively. Reproduced with permission from ref. 19. Copyright 2015, Springer International Publishing AG.

3.2 Platinum

Inspired by the repeated growth of graphene on Pt foils, h-BN syntheses on Pt have been targetedly attempted. A pioneer study by Shin's research team at the Ulsan National Institute of Science and Technology demonstrated the large-area growth of high-quality h-BN monolayer on recyclable Pt foil by an LPCVD method.[15] The use of Pt allowed the as-grown h-BN film to be intactly delaminated *via* electrochemical bubbling transfer (illustrated in **Fig. 7a**), thereby bypassing the use of hazardous etchants and reducing the costs of substrate loss. After transferred onto SiO_2/Si substrate, monolayer h-BN was characterised by OM and SEM (**Fig. 7b and c**). Furthermore, an aberration-corrected TEM operated at 80 kV was employed to observe the atomic structure of monolayer h-BN, as shown in **Fig. 7d**. It was claimed that the quality of the grown h-BN layers showed no significant degradation even after 100 growth cycles.

Similar to the growth on Cu, the layer number of h-BN grown on Pt surface was seen to alter with chamber pressure and BN source concentration. In general, at low pressure, the growth was self-limited to monolayer. However, the layer number would increase from monolayer to few-layer with the increase of precursor dosage within an APCVD process, as witnessed by Gao *et al*.[16] In their study, monolayer and bilayer h-BN domains can be selectively obtained on Pt by simply tuning the concentration of precursor (**Fig. 7e and f**), which is one of the advantages of APCVD on Pt foils over other methods for h-BN growth. In addition, repeated use of Pt substrates can be realized with the aid of a bubbling transfer method.

It is worth-mentioning that high-quality 2D h-BN was also successfully prepared on Pt surface by using liquid-phase borazine as the source.[29] In the experimental set-up, liquid borazine was filled into a bubbler, which was kept at a temperature of -10°C in a chiller to avoid the self-decomposition of the borazine. Hydrogen was purged through the bubbler to supply the vaporized borazine into the reactor chamber (**Fig. 7g**). It was found that the borazine source was more favourable than solid-phase ammonia borane since the solid precursor would lead to the deposition of undesirable BN particles by thermal activation during growth, thereby compromising the quality and purity of as-grown h-BN layers.[29]

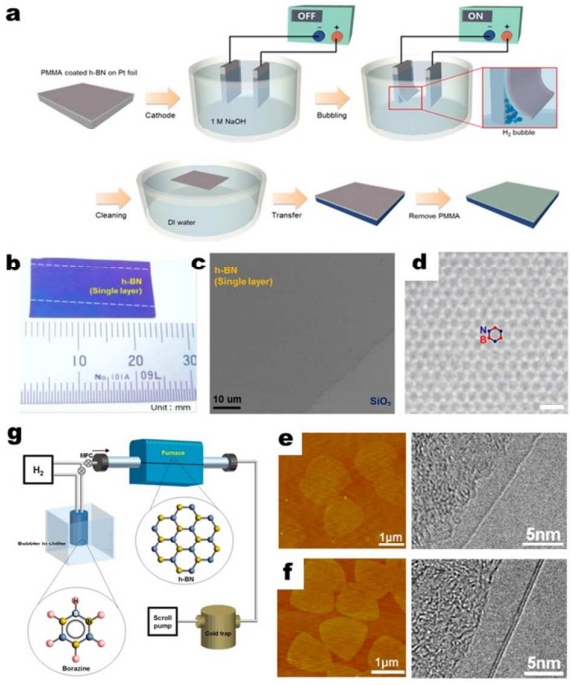

Fig. 7 h-BN growth on Pt substrates. (a) Schematic diagram of the electrochemical bubbling-based route used to transfer the h-BN layer grown on Pt, highlighting the

recycling of the Pt foil. (b) Photograph of an h-BN monolayer transferred onto a SiO_2/Si substrate. (c) SEM image of the monolayer h-BN film. (d) Atomically resolved TEM image of the monolayer h-BN. Scale bar, 1 nm. Reproduced with permission from ref. 15. Copyright 2013, American Chemical Society. (e and f) AFM and TEM characterisation of monolayer and bilayer h-BN grown on recyclable Pt substrate. Reproduced with permission from ref. 16. Copyright 2013, American Chemical Society. (g) Schematic diagram of LPCVD setup equipped with a bubbler using liquid borazine precursor to grow monolayer h-BN film on Pt. Reproduced with permission from ref. 29. Copyright 2014, American Chemical Society.

3.3 Nickel

An early investigation on the growth of 2D h-BN films on Ni substrate was reported by Jing Kong's research group from Massachusetts Institute of Technology.[10] Their study demonstrated the use of APCVD to synthesize large-area h-BN films (5-50 nm thickness) on polycrystalline Ni with borazine serving as the BN source. It is evident from OM and AFM observations that the film is homogeneous on each Ni facet, whilst along the grain boundaries the layer becomes noticeably thicker (**Fig. 8a and b**). High-magnified TEM measurement manifests that the interlayer distance of obtained thin film is around 0.35 ± 0.02 nm, indicative of the successful preparation of few-layer h-BN (**Fig. 8c**).

Interestingly, the growth of h-BN films on polycrystalline Ni substrates exhibited apparent Ni facet selectivity, as probed by Lee *et al.*[30] By employing OM, EBSD mapping and Raman spectroscopy, the effect of underlying Ni crystal orientations on the growth behaviour of h-BN layers produced by LPCVD was studied in detail (**Fig. 8d**). It was found that the growth rate of h-BN was prominent on Ni (100) facets but negligible on Ni (111) facets, implying that kinetic rather than thermodynamic control for the CVD growth of h-BN on Ni should be taken into consideration. It is worth-mentioning that such a substrate-facet-selective growth of h-BN was also observed by using Pt.[29]

In turn, tailored synthesis of h-BN films with uniform thickness and large-area flatness marks a great step forward in the development of techniques. With respect to Ni serving as the growth substrate, the thickness-dictated synthesis has been recently realized by Oh *et al.* on Ni (111) single crystals.[31] In this sense, a refined APCVD protocol by using optimal source sublimation and growth temperatures was employed (**Fig. 8e**), enabling the recyclable growth and transfer of centimetre-sized, epitaxial h-BN few-layer films. The uniform h-BN films can be of 2 × 2 cm^2 size (**Fig. 8f**), possessing uniform thickness at the nanometre scale over the entire region. Of particular note, the Ni substrate was reusable and uniform h-BN films could be reliably reproduced (**Fig. 8g**). This controlled growth of high-quality h-BN films in a recyclable fashion marked a great progress on 2D h-BN synthesis on Ni, in sharp contrast to the previously reported growth on poly-crystalline Ni foils, which often gave rise to multiple h-BN patches with varying thickness.

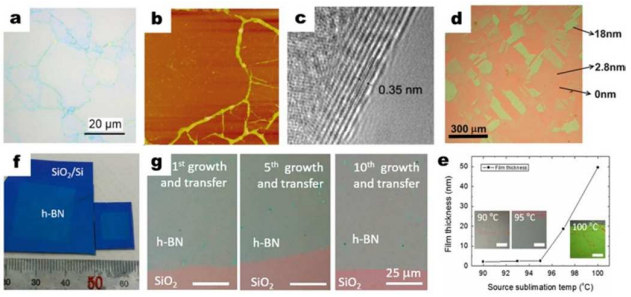

Fig. 8 h-BN growth on Ni substrates. (a) OM image of a h-BN film transferred from Ni onto a SiO_2/Si substrate. (b) AFM image of a transferred h-BN film. The image size is 20 μm × 20 μm. (c) TEM image showing the few-layer thickness of obtained h-BN films. Reproduced with permission from ref. 10. Copyright 2010, American Chemical Society. (d) OM image of h-BN films transferred onto a SiO_2/Si substrate, showing facet-selective growth behaviour. Reproduced with permission from ref. 30. Copyright 2012, Royal Society of Chemistry. (e) Thickness of h-BN films grown at different precursor sublimation temperatures. Insets: OM images of the obtained h-BN film on SiO_2/Si substrates. Scale bars, 50 μm. (f) Photograph of centimetre-scale h-BN film. (g) OM images of h-BN films obtained from the same Ni (111) substrate with repeated use of the substrate. Reproduced with permission from ref. 31. Copyright 2016, Nature Publishing Group.

3.4 Iron

For practical applications of h-BN such as dielectric layers and insulating membranes, it has been well recognized that multilayer film with uniform thickness of ~5-15 nm is highly desirable. Although uniform growth of few-layer was readily achieved on expensive Ni (111) single crystals as aforementioned, large-area, high-quality h-BN films produced on a cost-effective substrate is otherwise more pivotal in advancing the high performance of nanoelectronic devices. Fe, in this respect, has been proven a good choice. Recently, Kim *et al.* presented a new approach for controllable and repeatable growth of multilayer h-BN films over Fe foils with the supply of borazine vapour and hydrogen at 1100°C (**Fig. 9a**).[32] The thickness of films can be dictated by the cooling rate of the sample. Fast cooling rate (30°C·min^{-1}) resulted in a relatively thin h-BN film (average thickness 11.9 nm) whereas a slow cooling rate (5°C·min^{-1}) gave rise to thicker layers (average thickness 17.8 nm). Based on the experimental results, the h-BN film might be generated *via* both surface-mediated growth and precipitation according to the report. The as-synthesized film was of high-crystallinity and multi-layer nature (**Fig. 9b**), with the surface flatness comparable with that of mechanical-exfoliated h-BN flake (**Fig. 9c**).

The Fe-catalysed growth of h-BN has indeed sparked research attentions in recent years, and to date it is even possible to grow highly controlled monolayer films on Fe *via* CVD. Caneva *et al.* has made great contribution to this research direction.[24, 33] In one of their recent studies, a designed maneuver by exposing Fe to NH_3 during pre-annealing prior to the actual growth step enabled great improvement in the homogeneity and layer number control for h-BN (**Fig. 9d**).[24] The pre-feeding of N species into the Fe bulk would limit the uptake of B and N species during precursor exposure and hence restrain the precipitation-driven growth to some extent. As such, NH_3 pre-annealing led to the

exclusive growth of monolayer h-BN, whereas non-uniform, multi-layer material was produced by conventional H_2 pre-annealing (**Fig. 9e**).

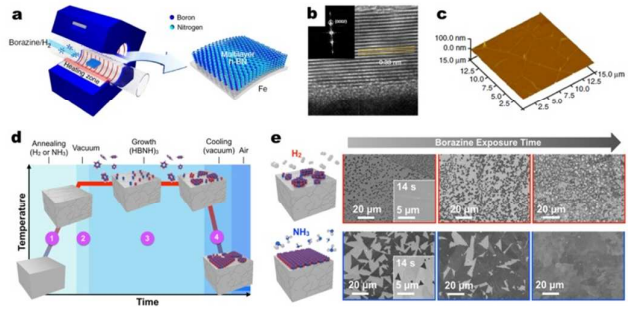

Fig. 9 h-BN growth on Fe substrates. (a) Schematic diagram of the LPCVD approach for multilayer h-BN synthesis on Fe foils. Borazine is used as a precursor. (b) HRTEM image of as-grown multilayer h-BN film on a Fe foil, identifying the (0002) lattice plane (inset) with a d-spacing of 0.33 nm. (c) AFM image of the multilayer h-BN film with a surface roughness value of ~0.2 nm. Reproduced with permission from ref. 32. Copyright 2015, Nature Publishing Group. (d) Schematic of the salient stages of the h-BN CVD process, where the pre-annealing stage in H_2 or NH_3 is marked. (e) SEM images of h-BN domains grown at 900 °C with borazine exposure, showing apparent advance when using NH_3-annealed Fe. Reproduced with permission from ref. 24. Copyright 2016, American Chemical Society.

3.5 Metal alloys

The growth of h-BN on metal alloys can bring us with unprecedented results mainly in terms of layer thickness uniformity and domain size enlargement. Zhang *et al.* designed a rational approach for the thickness-controlled synthesis of 2D h-BN thin films *via* the co-segregation of boron and nitrogen atoms from a Fe-Ni alloy.[17] To better control the segregation process, a sandwiched substrate with a solid-state (B, N)-interlayer between an Fe top layer and a Ni bottom layer was primarily fabricated. Upon vacuum annealing, pre-dissolved B and N automatically co-segregate from the bulk to the substrate surface, thereby forming h-BN films (**Fig. 10a**). The thickness of the h-BN films can be tailored by controlling the thickness of the Fe layer, which decreases linearly as the thickness of the Fe increases (**Fig. 10b and c**). Such a co-segregation strategy opened up a novel pathway for batch production of wafer-scale h-BN thin films with controlled layer thickness (**Fig. 10d**).

It is well known that Cu-Ni alloy is an ideal platform for the successful CVD synthesis of inch-sized graphene single crystals.[34] Very recently, Lu *et al.* continued their successful exploration by demonstrating that such an alloy was also suitable for the growth of large single-crystalline h-BN domains.[20] The synthetic procedure was quite straightforward, including the rational design of Cu-Ni substrate and LPCVD process of h-BN formation (**Fig. 10e**). Time-dependent growth investigations on alloy substrates with 15 atom% Ni clearly show that the h-BN domains grow up and finally coalesce into a continuous film (**Fig. 10f-h**). It was found that on Cu-Ni alloy the h-BN nucleation density can be greatly reduced to 60 per mm^2, and the single-crystal h-BN domains can expand as surprisingly large as 7500 μm^2 under optimised conditions. By further probing the influence of Ni concentration on h-BN growth, the authors claimed that Ni could enhance the decomposition of poly-aminoborane, leading to the production of high-quality h-BN grains on Cu-Ni alloys (**Fig. 10i**).

In this part, a series of major works involving the growth of h-BN on metals that have been identified as promising growth substrates are discussed. It is pivotal to have insights into the h-BN growth on metals at the atomic level. In general, the CVD growth of h-BN on metals can be realized with the following steps: i) sublimation (evaporation) of solid (liquid) BN precursors and gas-phase transportation; ii) adsorption and catalytic decomposition of (B, N)-containing species on metal surfaces; iii) diffusion of (B, N) radicals into or on metals; and iv) nucleation and further 2D growth. The rational CVD synthesis of h-BN films with large domain size, low defect density and high flatness requires a smooth metal substrate surface, tailored operating pressure/temperature and surface pre-treatment to minimize the nucleation density, as well as fine tune of precursor/carrier gas ratios in order to augment the growth rate.

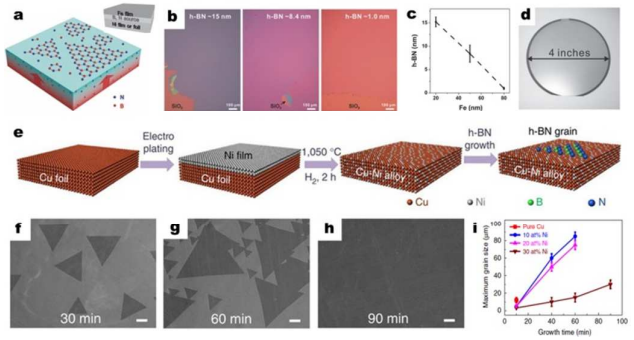

Fig. 10 h-BN growth on metal alloy. (a) Schematic of h-BN synthesis by the vacuum annealing of sandwiched Fe/(B, N)/Ni substrates. (b) OM images of as-grown h-BN thin films grown using Fe layers with different thicknesses. (c) Thickness of h-BN thin films as a function of Fe thickness. (d) Photograph of a monolayer h-BN film with 4-inch wafer scale prepared by the co-segregation method. Reproduced with permission from ref. 17. Copyright 2014, Wiley-VCH. (e) Schematic illustration showing the procedure of large single-crystal h-BN growth on Cu-Ni alloy. (f-h) Typical SEM images of h-BN domains grown on Cu-Ni alloy foils with 15 atom% Ni at 1085 °C for 30, 60 and 90 min, respectively. Scale bars, 20 μm. (i) Dependence of the maximum h-BN domain size on Ni concentration and growth time. Reproduced with permission from ref. 20. Copyright 2015, Nature Publishing Group.

4. Controllable growth of h-BN on dielectrics

Catalyst-free synthesis of 2D h-BN on desired dielectric substrates in a controllable manner is of great significance as it not only bypasses tedious transfer processes but also facilitates direct device integration and applications. While it was questionable several years ago to directly fabricate 2D h-BN over dielectrics due to the nature of limited catalytic activity of substrates, recent experimental attempts have indicated that this is not a problematic issue. Several strategies have been developed to manipulate the nucleation and growth process of h-BN on dielectric surface, resulting in a great deal of control over the as-obtained h-BN qualities and properties. However, a common sense is that it is more

difficult to tailor the h-BN nucleation density and the growth kinetics on dielectrics as compared to metal substrates, and the sizes of h-BN crystal domains normally fall into nanometre regime. This section will deal with the latest advances in direct growth of 2D h-BN on conventional insulators.

4.1 Early attempts

Early investigations on the h-BN growth over dielectric layers have typically centred on testing the growth feasibility by simple metal-free CVD routes, that is, on addressing the concern regarding "whether can grow" instead of "how to grow". In 2011, Kim *et al.* pioneered in attempting the deposition of h-BN directly on non-catalytic surfaces such as Si (001) and Al_2O_3 (0001) by thermal CVD.[11] The experimental results showed that a crystalline few-layer h-BN film can be grown on Al_2O_3 at 1000°C by controlling the flow kinetics (**Fig. 11a and b**), whereas Si substrate enabled no growth at all. The breakthrough attained in this study is quite important for the field of h-BN synthesis.

Following this success, Tay *et al.* demonstrated a metal-free CVD approach to fabricate few-layer nanocrystalline h-BN on amorphous SiO_2/Si and quartz substrates (**Fig. 11c**).[35] Due to the absence of catalytic metals at the growth stage, an elevated synthetic temperature was required to surmount the higher activation energy for achieving a successful growth. The as-grown film was smooth and free of observable wrinkles (**Fig. 11d**). The whole growth was without metal assistance, as XPS characterisation showed no trace of Cu and other metallic contaminations (**Fig. 11e**). The formation of few-layer h-BN film was witnessed by TEM (**Fig. 11f**), but the lateral sizes of h-BN domains were quite small because of the random and uncontrolled nucleation of h-BN on SiO_2 substrates.

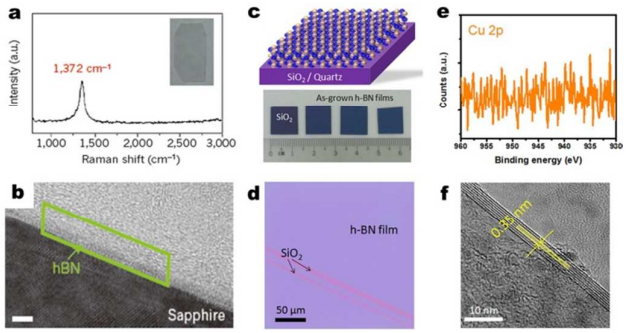

Fig. 11 Early-stage investigations on direct growth of h-BN over dielectrics. (a) Raman spectrum of h-BN film grown on Al_2O_3 (0001) substrate, showing a typical Raman peak at 1372 cm^{-1}. Inset: h-BN sample grown on the Al_2O_3 (0001) substrate. (b) TEM image showing the direct coating of h-BN. Reproduced with permission from ref. 11. Copyright 2011, Nature Publishing Group. (c) Schematic diagram and photograph of direct-grown nanocrystalline h-BN films on SiO_2/Si substrates. (d) OM image of as-grown h-BN film with a scratched region exposing the underlying SiO_2 surface. (e) Magnified XPS Cu 2p spectrum showing no trace of Cu. (f) TEM image taken at a folded edge showing the layer number of directly grown h-BN film. Reproduced with permission from ref. 35. Copyright 2015, AIP Publishing LLC.

4.2 Further developments

Recently, further key efforts have been made to rationally design the growth protocols, aiming to gain fine controls over the direct CVD process for realizing h-BN production with better quality. The h-BN nucleation stage can be tailored by modifying the surface features of dielectric substrates. Inspired by the oxygen-assisted, catalyst-free graphene growth,[36] Behura *et al.* presented a new boron-oxygen chemistry route to realize oxygen-aided nucleation of h-BN, leading to the preparation of large-area, uniform h-BN directly on piranha-treated SiO_2 substrates (**Fig. 12a**).[21] It is noted in this study that an LPCVD process was employed, making the growth of thickness-uniform h-BN film applicable (**Fig. 12b**). XPS measurements clearly revealed the existence of B-O bonding but showed no sign of N-O bonding (**Fig. 12c**), suggesting the nucleation of h-BN domains commenced when boron radicals bound at the oxygen dangling bond of SiO_2. Moreover, control experiments using Si displayed no growth of h-BN, indicating the importance of oxygen groups on the substrate. Specifically, the directly-obtained h-BN film presented an ultra-smooth surface, showing a 6.27-fold reduced surface roughness as compared to that of SiO_2 (**Fig. 12d**).

The field of direct synthesis of h-BN on insulators has been greatly advanced by Jang's recent work on the epitaxial growth of wafer-scale, wrinkle-free, single-crystalline, few-layer h-BN on a sapphire (c-plane) substrate.[23] Such a high-quality h-BN thin film was realized by a high-temperature and low-pressure CVD reaction, where the growth temperature was normally at 1400°C (**Fig. 12e**). Control experiments confirmed that high temperature was imperative for the epitaxial growth of h-BN, owing to the negligible catalytic effect of sapphire. The 2-inch-wafer scale, high crystallinity h-BN film was also featured by its highly smooth surface without any wrinkle structures, possessing a surface roughness value (0.169 nm) much smaller than that of h-BN grown on Pt (1.09 nm) (**Fig. 12f-h**). Investigation on the epitaxial orientation of h-BN on sapphire by low-energy electron diffraction (LEED) and DFT calculation indicated that R30° was the preferred orientation angle (**Fig. 12i**). While the h-BN film grown on sapphire was of large-scale and high-quality, a transfer process was still necessary, enabling the reusability of the sapphire substrate. **Table 1** summarizes the CVD growth routes and product features of 2D h-BN materials synthesized on various substrates reviewed in this article.

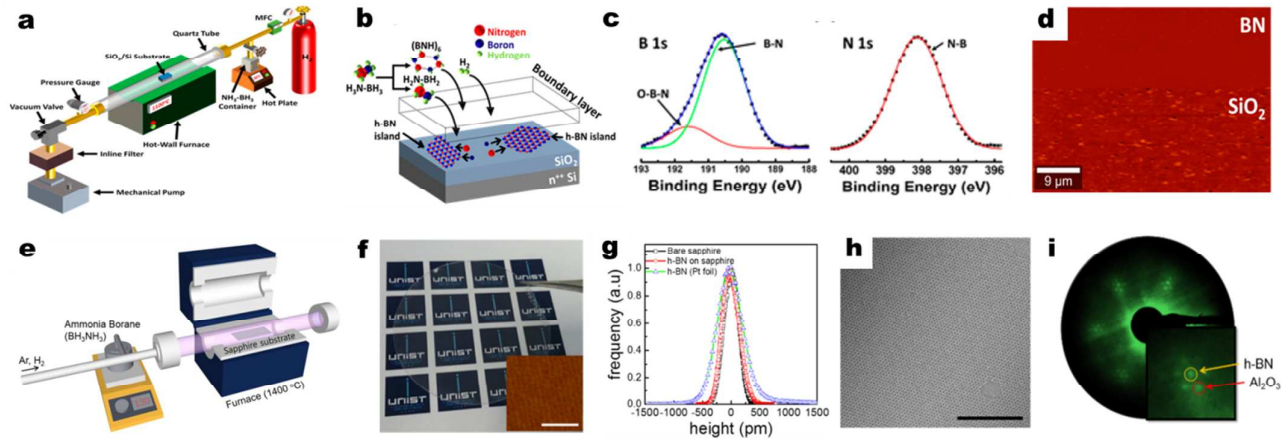

Fig. 12 Protocol design with respect to the direct growth of h-BN on dielectrics. (a) CVD system setup for the oxygen-aided, transfer-free growth of h-BN on SiO_2/Si substrates. (b) Schematic for the proposed growth mechanism. (c) XPS analysis for B 1s and N 1s, where the B-O peak indicates the presence of boron terminated edges bonded to SiO_2. (d) AFM image of SiO_2/Si before and after h-BN growth, showing much decreased density of absorbed impurities and a smooth surface of h-BN. Reproduced with permission from ref. 21. Copyright 2015, American Chemical Society. (e) Schematic of the LPCVD system used for few-layer h-BN growth on sapphire substrate at high temperatures. (f) A photograph of wafer-scale h-BN directly-grown on sapphire substrate. Inset: Corresponding AFM image showing a highly smooth surface. Scale bar, 500 nm. (g) Histogram of the height distribution (surface roughness) of h-BN grown on sapphire and on Pt foil. (h) HRTEM image of AA' stacked h-BN. Scale bar, 5 nm. (i) LEED pattern of single-oriented h-BN grown on sapphire substrate at 120 eV. Reproduced with permission from ref. 23. Copyright 2016, American Chemical Society.

Table 1 A summary of growth methods and features of 2D h-BN synthesized on various substrates by CVD

Substrate	CVD route	Growth temp. (°C)	Precursor	Layer No.	Single domain (μm^2)	E_g (eV)	Key parameter	Ref.
Cu foil	APCVD	1000	ammonia borane	2-5 layers	-	5.56	-	9
Cu foil	APCVD	1000	ammonia borane	6-8 layers	-	-	Cu morphology	14
Cu foil	LPCVD	1000	ammonia borane	monolayer	0.5	6.07	-	13
Cu/SiO_2/Si	PECVD	800	borazine	few-layers	-	5.47	Growth temp. and time	18
Cu foil	APCVD	1050	ammonia borane	monolayer	35	6.04	Surface smooth	27
Cu foil	LPCVD	1000	ammonia borane	monolayer	170	-	Cu pretreatment	22
Cu foil	LPCVD	1000	ammonia borane	monolayer	2200	5.9	Using Cu enclosure	19
Cu foil	APCVD	1065	ammonia borane	monolayer	170	5.85	Synthetic control	26
Ni film	APCVD	1000	borazine	5-50 nm	-	5.92	Precursor dosage	10
Ni (111)	APCVD	800-1030	ammonia borane	few-layers	-	-	Repeated growth	31
Pt foil	LPCVD	1100	ammonia borane	monolayer	-	6.06	Repeated growth	15
Pt foil	APCVD	1000	ammonia borane	1-3 layers	0.5 (for monolayer)	6.07 (1L), 5.94 (2L)	Repeated growth with layer controllability	16
Fe foil	LPCVD	1100	borazine	5-15 nm	-	-	Furnace cooling rate	32
Fe foil	LPCVD (cold-wall)	900	borazine	monolayer	170	-	NH_3 pre-annealing	24
Fe-Ni	LPCVD	900-1100	B,N-solid source	monolayer, few-layers	-	5.8	Co-segregation	17
Cu-Ni	LPCVD	1050-1085	ammonia borane	monolayer	7500	-	Tuning Ni dosage	20
SiO_2	LPCVD	1000	ammonia borane	few-layers	nanosized	6.03	Growth time	35
SiO_2, quartz	LPCVD	1000	ammonia borane	few-layers	-	5.51	O-assisted nucleation and growth	21
sapphire	LPCVD	1400	ammonia borane	few-layers	-	5.75	Epitaxial growth	23

5. h-BN serving as a 2D growth substrate

The world of 2D heterostructures continues to expand at a faster rate than ever expected, leading to a plethora of new excitement in materials science and nanotechnology. In fact, one important impetus behind the 2D heterostructure research was concerned with the reduction of charge puddles in graphene, where h-BN was proven an excellent platform for graphene electronics.[5] However, the creation of 2D heterostructures *via* sequential transfer of exfoliated flakes poses several limitations, such as lack of scalable production,

poor position control, contamination at the interface, and tedious fabrication process. In this regard, the direct growth of vertically stacked 2D heterostructures by CVD is much more attractive in terms of scalability, controllability and feasibility. More specifically, growing 2D materials on insulating h-BN sheets is critical for a variety of device applications. In this part, we will present recent advance in direct synthesis of 2D heterostructures using CVD-derived h-BN as a 2D growth substrate. The growth scenarios based upon mechanical exfoliated h-BN flakes will not be addressed here as they normally possess limited sizes as well as have not employed "all-CVD" route for the 2D heterostructure production.

5.1 h-BN as a substrate for graphene growth

h-BN has emerged as a highly versatile platform as a barrier-, protection-, or support-layer for graphene electronics and optoelectronics. The direct growth of vertically-stacked graphene/h-BN heterostructures has accordingly stimulated great research interests. An early effort made by Wang *et al.* dealt with a two-step CVD route to obtain graphene/h-BN stacks through sequentially synthesizing graphene and h-BN on Cu foils (**Fig. 13a-c**).[37] By conducting systematic carrier transport measurements, they managed to demonstrate the capability of scalable production of graphene/h-BN heterostructures with a tight and clean interface demanded for high-performance graphene devices.

A current strong interest has been focused on the one-batch CVD synthesis of vertical graphene/h-BN hybrids due to the processing controllability and simplicity. Zhongfan Liu's group from Peking University is a pioneer in this research direction. In 2015, they developed a temperature-triggered, chemical switching LPCVD route for the one-batch growth of graphene/h-BN heterostructures on Cu foils.[38] The use of a specific carbon precursor, benzoic acid, enabled the growth of graphene on h-BN at a relatively low growth temperature (<900°C), thereby circumventing the etching of the pre-deposited h-BN (**Fig. 13d**). In this sense, discrete graphene islands and fully-covered monolayer films can be realized by controlling the growth parameter such as deposition time and carbon feeding rate (**Fig. 13e and f**). Although wafer-scale graphene/h-BN heterostructures were successfully prepared (**Fig. 13g**), the nucleation sites, domain sizes and stacking geometries of graphene on h-BN remained uncontrollable.

They also demonstrated a seed-assisted CVD route for tailored synthesis of patterned single-crystalline graphene/h-BN vertical stacks.[39] By introducing pre-defined seed on Cu foils prior to the CVD growth, the domain location and quality of graphene can be controlled. More significantly, the nucleation density and domain size of graphene/h-BN heterostructures were simply tuned by altering the interspace of seeds, achieving the growth of isolated graphene domains as well as complete films on h-BN (**Fig. 13h-l**). This seed-assisted CVD technique extends the research frontier on 2D heterostructure growth and opens up new path to the development of their advanced applications. Further, with respect to the fast growth of graphene domains on h-BN film, recently they managed to present a metal-atom-facilitated sequential CVD route for the direct synthesis of graphene/h-BN stacks using nickelocene as the carbon precursor, realizing an improved synthesis efficiency (8-10 times faster) as well as crystalline quality of graphene (domain sizes up to ~20 μm).[40] For these studies employing Cu as underlying substrates, the growth mechanism of graphene on h-BN/Cu is differentiated from that on bare h-BN. In such cases, catalytic transparency of h-BN is indeed an insteresting issue and waits to be further unravelled to better understand the growth details.

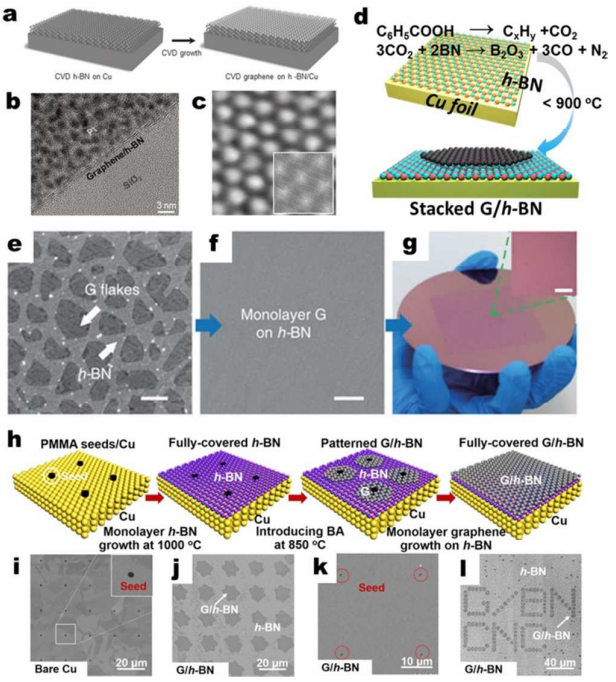

Fig. 13 CVD-derived h-BN serving as a 2D substrate for graphene growth. (a) Schematic of graphene directly grown on CVD h-BN film/Cu foil. (b) Cross-sectional TEM image of a CVD-grown graphene/h-BN film transferred onto a SiO_2/Si substrate. (c) STM image showing the Moiré pattern of 4.2 nm period. Image area: 23 nm × 23 nm. Reproduced with permission from ref. 37. Copyright 2013, Wiley-VCH. (d) Schematic illustration showing stacked graphene/h-BN heterostructures can be obtained below 900 °C using benzoic acid as the carbon precursor. (e and f) SEM images of h-BN partially and fully covered by graphene, respectively. Scale bar, 1 μm (e) and 2 μm (f). (g) Photograph of the wafer-scale graphene/h-BN film transferred onto SiO_2/Si substrate. Inset: An OM image. Scale bar, 20 μm. Reproduced with permission from ref. 38. Copyright 2015, Nature Publishing Group. (h) Schematic diagram of key steps in the growth of patterned graphene/h-BN domains and monolayers using pre-deposited seeds on Cu foils as nucleation sites. (i-l) SEM image library showing the pre-defined seed on bare Cu, patterned graphene domains grown on h-BN, fully-covered graphene/h-BN films and patterned graphene/h-BN domains, respectively. Reproduced with permission from ref. 39. Copyright 2016, American Chemical Society.

5.2 h-BN as a substrate for other 2D material growth

Being a chemically-inert and electrically-insulating 2D flatland, h-BN is featured by its atomically flat surface without dangling bonds and charged impurities, which would greatly advance the device performances of 2D van der Waals (vdW) solids. As such, h-BN serves as a growth template for the direct deposition of 2D atomic crystals beyond graphene, including TMDs and organic perovskites. Recently a great deal of efforts

has been devoted to grow 2D materials *via* CVD on mechanically exfoliated h-BN flakes, forming various 2D vertical heterostructures, such as MoS_2/h-BN,[41] WS_2/h-BN,[42] ZrS_2/h-BN[43] and so on. More essentially, "all CVD" route leading to the build-up of large-area vdW heterostructures is on the rise.

With respect to all-CVD-derived TMDs/h-BN layers, a few attempts have been made to date, either *via* a transfer-growth route[44] or by means of one-batch synthetic method.[21, 45] A representative study by Lei Fu's research team at Wuhan University utilized a sulfide-resistant Ni-Ga alloy to achieve the direct CVD growth of MoS_2/h-BN vdW heterostructures without any intermediate transfer steps.[46] In this work, a Mo foil served as both the support beneath the Ni-Ga alloy and the Mo source for MoS_2 growth (**Fig. 14a**). The sulfide-resistant performance of the Ni-Ga alloy was investigated by XPS depth profiles and DFT calculations. The as-grown heterostructure was of high-quality according to systematic characterisations, realizing large-sized (up to 200 μm^2) MoS_2 single crystals on h-BN (**Fig. 14b-d**). Such a route is potential to be extended as a universal approach for direct growth of various novel 2D heterostructures.

Recently, Niu *et al.* reported the direct production of large-scale organic/inorganic vdW heterostructures, where organic perovskite $CH_3NH_3PbI_3$ nanoplatelets were deposited on h-BN (**Fig. 14e-g**) and other 2D inorganic substrates.[47] The construction of vdW heterostructures with a clean interface offered great opportunity to tune the light-matter interactions. In particular, this study demonstrated that h-BN monolayer was a suitable platform to organic perovskites for preserving their original optical properties, where the patterned organic perovskite/h-BN vdW hybrids showed excellent light emission performance.

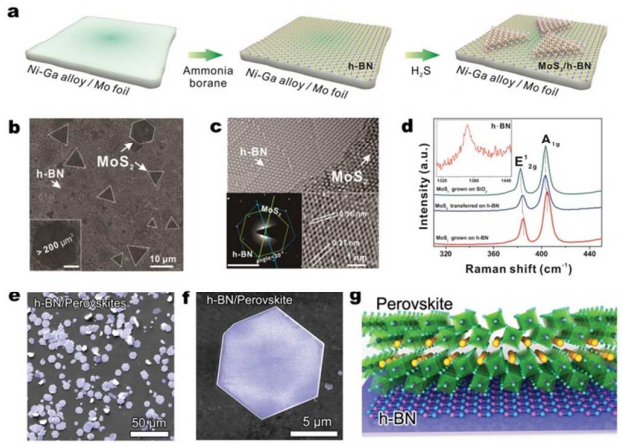

Fig. 14 CVD-derived h-BN as a 2D substrate for growing 2D material beyond graphene. (a) Schematic showing the preparation of MoS_2/h-BN heterostructure. (b) SEM image of the directly grown single-crystal MoS_2 on h-BN. Inset: MoS_2 crystal with grain size up to 200 μm^2. Scale bar, 5 μm. (c) TEM image of MoS_2/h-BN heterostructures. Inset: Corresponding SAED patterns. Scale bar, 0.2 nm. (d) Raman spectra collected from different MoS_2/h-BN samples. Reproduced with permission from ref. 46. Copyright 2016, American Chemical Society. (e and f) Low- and high-magnified false-coloured SEM images of perovskite 2D vdW solids (light blue) grown on h-BN films. (g) Structure model of 2D perovskite/h-BN heterostructures. Reproduced with permission from ref. 47. Copyright 2015, Wiley-VCH.

6. Device applications of CVD-derived h-BN

2D h-BN material has triggered wide attention for practical applications nowadays due to its excellent electrical insulation, high thermal conductivity, superb oxidation resistance and compatibility with 2D device integration. In particular, CVD-derived h-BN films, featured by high-quality and large-scale, are highly desirable for various applications. The most promising application is their use as dielectric layers in graphene electronic devices. Furthermore, h-BN sheets grown *via* CVD can be utilized as chemically-stable, high-temperature coatings, robust heat dissipation films, cation mobility reduction barriers in flexible resistive memory devices, effective electron-blocking/hole-transporting layers in solar cells *etc.* This section presents an overview of key device applications of CVD-derived 2D h-BN films.

6.1 Dielectrics for advanced graphene electronics

h-BN layer has been deemed as an ideal candidate as gating material for graphene electronic devices. Even monolayer h-BN can be used as a dielectric substrate. By using one-batch CVD method, Gao *et al.* successfully prepared monolayer graphene single-crystalline domain/monolayer h-BN film on Cu foils (**Fig. 15a**).[38] TEM characterisations substantiated that this heterostructure was composed of bare two layers (**Fig. 15b and c**). Further transferring the as-grown hybrid onto SiO_2/Si substrate facilitated the fabrication of a field effect transistor (FET) device (**Fig. 15d**), which demonstrated a carrier mobility of 15000 $cm^2 \cdot V^{-1} \cdot s^{-1}$ at room temperature (**Fig. 15e**).

Compared to monolayer h-BN, few-layer even multi-layer films are considered to be more suitable for use as dielectrics and/or barriers, the thickness of which guarantees excellent dielectric properties with a low leakage current, as well as sufficient room for blocking the scattering effects from underlying impurities. To this end, synthesizing multi-layer h-BN film at a large area by CVD on low-cost Fe foils is indeed meaningful. The thickness of obtained h-BN film was in the range of 5-15 nm (**Fig. 15f**), and the reported graphene mobility reached 24000 $cm^2 \cdot V^{-1} \cdot s^{-1}$ at room temperature, outperforming that achieved with bare SiO_2-based devices (**Fig. 15g-i**).[32]

In 2016, the dielectric capability of high-quality h-BN films directly grown on sapphire substrate was also demonstrated. The few-layer, wafer-sized h-BN film was transferred on 300 nm thick SiO_2/Si for fabricating back-gated graphene FET arrays.[23] The measured values of electron and hole mobility in graphene on h-BN/SiO_2 were 14175 and 8670 $cm^2 \cdot V^{-1} \cdot s^{-1}$, respectively. These values were comparable with graphene on mechanically exfoliated h-BN, and superior to those on SiO_2 (**Fig. 15j-m**). It is also worth-noting that h-BN layers enabled efficient prevention of p-doping effect of graphene from the SiO_2 substrate, thereby improving the electron mobility. These studies suggest that CVD-derived h-BN is readily useful as a large-area insulating substrate for graphene electronics.

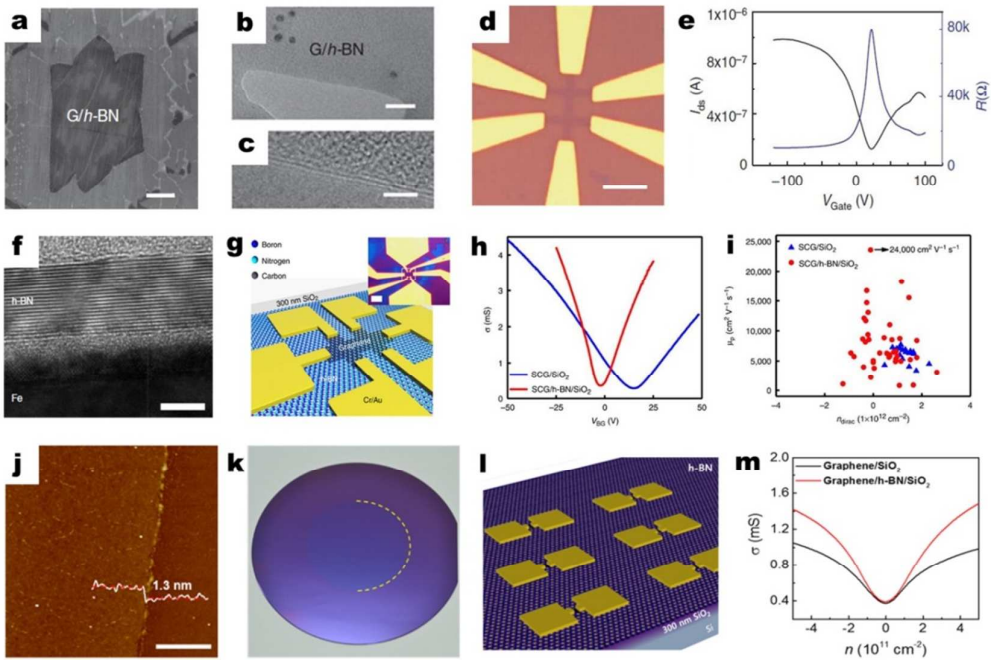

Fig. 15 Device applications of CVD-derived h-BN in terms of advancing graphene electronics. (a) SEM image of large-sized graphene domain grown on h-BN. Scale bar, 5 μm. (b and c) Magnified TEM images of graphene/h-BN stacked film along the film edges showing monolayer graphene and monolayer h-BN. Scale bars, 20 nm (b) and 2 nm (c). (d) OM image of graphene back-gated FET fabricated on 300nm SiO_2/Si. Scale bar, 20 μm. (e) Device drain current (I_{ds}) and resistance (R) versus gate voltage (V_{gate}). Reproduced with permission from ref. 38. Copyright 2015, Nature Publishing Group. (f) Cross-sectional TEM image of an as-grown multilayer h-BN film on a Fe foil. Scale bar, 5 nm. (g) Schematic diagram of graphene FET on h-BN, with the inset showing the OM image of a real device. Scale bar, 10 μm. (h) Conductance (σ) of the graphene channel as a function of applied back gate (V_{BG}) at room temperature on SiO_2 (blue) and on h-BN/SiO_2 (red) substrates. (i) Plot of the extracted hole mobility (μ_p) vs. n_{dirac} for both of the substrates (h-BN and SiO_2). Reproduced with permission from ref. 32. Copyright 2015, Nature Publishing Group. (j) AFM image of transferred few-layer h-BN grown on sapphire substrate. Scale bar, 500 nm. (k) Photograph of a 2-inch h-BN sheet transferred onto a 4-inch SiO_2/Si wafer. (l) Schematic diagram of graphene FETs on h-BN/SiO_2/Si substrate. (m) Conductance (σ) of graphene FETs on bare SiO_2/Si and on transferred h-BN/SiO_2/Si as a function of carrier density. Reproduced with permission from ref. 23. Copyright 2016, American Chemical Society.

6.2 Other functional applications

Being large-scale and low-cost, CVD-derived 2D h-BN materials have endowed them with functional properties in a wide range of device applications. In 2013, Liu *et al.* demonstrated that ultrathin h-BN layers can be used as high-performance coatings on metals (such as stainless steel) to resist oxidation up to 1100°C, as witnessed in **Fig. 16a and b**.[48] Moreover, h-BN can also be coated on graphene, which showed retained graphene Raman signals even at a high temperature of 1000°C, confirming the protective nature of h-BN (**Fig. 16c**). Qian *et al.* constructed flexible h-BN based resistive switching memory devices and found that such devices demonstrated excellent performances in terms of retention time and bending endurance (**Fig. 16d and e**).[49] It was further shown that the resistive switching characteristics were governed by the h-BN, *i.e.*, the low cation mobility offered by the h-BN thin film. Very recently, Meng *et al.* introduced few-layer h-BN to engineer the graphene/Si interface within a solar cell configuration (**Fig. 16f**), achieving improved device performances.[50] According to their study, such an improvement was attributed to the fact that h-BN acted as an effective electron-blocking/hole-transporting interlayer, and in turn suppressed the interface recombination of carriers, as well as increased the conductivity of supported graphene (**Fig. 16g**).

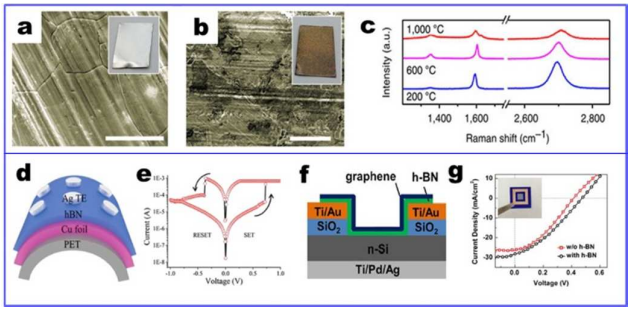

Fig. 16 Device applications of CVD-derived h-BN in terms of other applications. (a and b) SEM images of stainless steel surface with (a) and without h-BN (b) coatings at up to 1100 °C for 30 min. Scale bars, 40 μm. Inset: Photo of samples showing stainless steel can maintain their original colour with h-BN coating. (c) Typical Raman spectra for the h-BN-coated graphene under 200, 600 and 1,000 °C, showing h-BN film serving as an anti-oxidation layer for graphene. Reproduced with permission from ref. 48. Copyright 2013, Nature Publishing Group. (d) Schematic of flexible resistive memory device based on Ag/h-BN/Cu foil on PET. (e) Switching characteristics for the h-BN memory device. Reproduced with permission from ref. 49. Copyright 2016, Wiley-VCH. (f) Schematic illustration of graphene/h-BN/Si solar cells. (g) Illuminated J-V characteristics of the graphene/Si solar cells with and without an h-BN interlayer. Inset: Photograph of the graphene/h-BN/Si solar cell with 0.09 cm^2 junction area. Reproduced with permission from ref. 50. Copyright 2016, Elsevier Ltd.

7. Summary and outlook

The future directions for the practical applications of 2D h-BN materials depend upon progress in the controlled production with large-area and high-quality. This can be in particular realized by CVD routes, where many advances have been achieved in recent years. This tutorial review has discussed the latest research achievements in terms of tailored synthesis of 2D h-BN on various substrates by means of CVD, and will conclude here with several key challenges and prospects in this exciting field:

i) Effective control over the thickness uniformity of as-grown h-BN remains difficult. The exploration of innovative catalyst systems, such as new metal alloys, may provide direction for obtaining uniform monolayer or few-layer h-BN films. Moreover, the elucidation of growth mechanisms of h-BN would be indeed helpful to the CVD processing control for realizing enhanced qualities of h-BN materials.

ii) Direct growth on the dielectric substrates would be rewarding with regards to the practical applications with economic needs. In this respect, further attention needs to be paid on the property and status of the dielectric substrates (i.e., SiO_2/Si) to allow direct device integration, since the substrates might get affected by experiencing the CVD reaction. Moreover, due to the absence of any metallic catalyst, PECVD is a promising technique to fabricate h-BN over dielectrics with lowering growth temperatures and this route should be explored further.

iii) *All-CVD-derived* vdW heterostructures based on h-BN is appealing. During the elevated-temperature growth of second layered material on h-BN, how to prevent h-BN from etching is significant for the quality of desired heterostructures. In the specific case of growing graphene/h-BN heterostructures, the exploration of proper carbon precursor and growth temperature could effectively circumvent the etching of h-BN.

iv) The commercial aspects of CVD-derived h-BN deserve to be captured. In practice, CVD h-BN with sufficient film quality ready for almost any potential applications can usually be produced at relatively high temperatures solely at the expense of high energy consumption. The price of CVD h-BN is also pertaining to the production volume and costs for film transfer (*i.e.*, from Cu foils). Novel batch production routes might be helpful to lower the price and scale-up the product.

Acknowledgements

This work was supported by the National Natural Science Foundation of China (51702225, 51675275, 21473119, 51520105003 and 51432002) and Jiangsu Youth Science Foundation (BK20170336). J.Y.S., C.L., Y.Z.S., Q.C.L., L.Z. and Z.F.L. acknowledge the support from Suzhou Key Laboratory for Advanced Carbon Materials and Wearable Energy Technologies, Suzhou, China. J.Y.S. acknowledges the support from the Thousand Youth Talents Plan of China. Q.Q.J. and J.K. acknowledge the support by the STC Center for Integrated Quantum Materials, US. NSF Grant No. DMR-1231319.

References

1. A. K. Geim and I. V. Grigorieva, *Nature*, 2013, **499**, 419-425.
2. K. S. Novoselov, A. Mishchenko, A. Carvalho and A. H. Castro Neto, *Science*, 2016, **353**, aac9439.
3. D. Akinwande, N. Petrone and J. Hone, *Nat. Commun.*, 2014, **5**, 5678.
4. A. Pakdel, Y. Bando and D. Golberg, *Chem. Soc. Rev.*, 2014, **43**, 934-959.
5. C. R. Dean, A. F. Young, I. Meric, C. Lee, L. Wang, S. Sorgenfrei, K. Watanabe, T. Taniguchi, P. Kim, K. L. Shepard and J. Hone, *Nat. Nanotechnol.*, 2010, **5**, 722-726.
6. L. Banszerus, M. Schmitz, S. Engels, M. Goldsche, K. Watanabe, T. Taniguchi, B. Beschoten and C. Stampfer, *Nano Lett.*, 2016, **16**, 1387-1391.
7. Z. Y. Cai, B. L. Liu, X. L. Zou and H. M. Cheng, *Chem. Rev.*, 2018, DOI: 10.1021/acs.chemrev.7b00536.
8. T. Takahashi, H. Itoh and A. Takeuchi, *J. Cryst. Growth* 1979, **47**, 245.
9. L. Song, L. Ci, H. Lu, P. B. Sorokin, C. Jin, J. Ni, A. G. Kvashnin, D. G. Kvashnin, J. Lou, B. I. Yakobson and P. M. Ajayan, *Nano Lett.*, 2010, **10**, 3209-3215.
10. Y. Shi, C. Hamsen, X. Jia, K. K. Kim, A. Reina, M. Hofmann, A. L. Hsu, K. Zhang, H. Li, Z.-Y. Juang, M. S. Dresselhaus, L.-J. Li and J. Kong, *Nano Lett.*, 2010, **10**, 4134-4139.
11. K. Kim, J.-Y. Choi, T. Kim, S.-H. Cho and H.-J. Chung, *Nature*, 2011, **479**, 338-344.
12. L. Qin, J. Yu, M. Li, F. Liu and X. Bai, *Nanotechnology*, 2011, **22**, 215602.
13. K. K. Kim, A. Hsu, X. Jia, S. M. Kim, Y. Shi, M. Hofmann, D. Nezich, J. F. Rodriguez-Nieva, M. Dresselhaus, T. Palacios and J. Kong, *Nano Lett.*, 2012, **12**, 161-166.
14. K. H. Lee, H.-J. Shin, J. Lee, I.-Y. Lee, G.-H. Kim, J.-Y. Choi and S.-W. Kim, *Nano Lett.*, 2012, **12**, 714-718.
15. G. Kim, A. R. Jang, H. Y. Jeong, Z. Lee, D. J. Kang and H. S. Shin, *Nano Lett.*, 2013, **13**, 1834-1839.
16. Y. Gao, W. Ren, T. Ma, Z. Liu, Y. Zhang, W.-B. Liu, L.-P. Ma, X. Ma and H.-M. Cheng, *ACS Nano*, 2013, **7**, 5199-5206.
17. C. Zhang, L. Fu, S. Zhao, Y. Zhou, H. Peng and Z. Liu, *Adv. Mater.*, 2014, **26**, 1776-1781.
18. K. Zhang, F. L. Yap, K. Li, C. T. Ng, L. J. Li and K. P. Loh, *Adv. Funct. Mater.*, 2014, **24**, 731-738.
19. X. Song, J. Gao, Y. Nie, T. Gao, J. Sun, D. Ma, Q. Li, Y. Chen, C. Jin, A. Bachmatiuk, M. Rümmeli, F. Ding, Y. Zhang and Z. Liu, *Nano Res.*, 2015, **8**, 3164-3176.
20. G. Lu, T. Wu, Q. Yuan, H. Wang, H. Wang, F. Ding, X. Xie and M. Jiang, *Nat. Commun.*, 2015, **6**, 6160.
21. S. Behura, P. Nguyen, S. Che, R. Debbarma and V. Berry, *J. Am. Chem. Soc.*, 2015, **137**, 13060-13065.
22. L. Wang, B. Wu, L. Jiang, J. Chen, Y. Li, W. Guo, P. Hu and Y. Liu, *Adv. Mater.*, 2015, **27**, 4858-4864.
23. A. R. Jang, S. Hong, C. Hyun, S. I. Yoon, G. Kim, H. Y. Jeong, T. J. Shin, S. O. Park, K. Wong, S. K. Kwak, N. Park, K. Yu, E. Choi, A. Mishchenko, F. Withers, K. S. Novoselov, H. Lim and H. S. Shin, *Nano Lett.*, 2016, **16**, 3360-3366.
24. S. Caneva, R. S. Weatherup, B. C. Bayer, R. Blume, A. Cabrero-Vilatela, P. Braeuninger-Weirner, M.-B. Martin, R. Wang, C. Baehtz, R. Schloegl, J. C. Meyer and S. Hofmann, *Nano Lett.*, 2016, **16**, 1250-1261.
25. J. C. Koepke, J. D. Wood, Y. Chen, S. W. Schmucker, X. Liu, N. N. Chang, L. Nienhaus, J. W. Do, E. A. Carrion, J. Hewaparakrama, A. Ranaarajan, I. Datye, R. Mehta, R. T.

Haasch, M. Gruebele, G. S. Girolami, E. Pop and J. W. Lyding, *Chem. Mater.*, 2016, **28**, 4169-4179.
26. Y. Stehle, H. M. Meyer, III, R. R. Unocic, M. Kidder, G. Polizos, P. G. Datskos, R. Jackson, S. N. Smirnov and I. V. Vlassiouk, *Chem. Mater.*, 2015, **27**, 8041-8047.
27. R. Y. Tay, M. H. Griep, G. Mallick, S. H. Tsang, R. S. Singh, T. Tumlin, E. H. T. Teo and S. P. Karna, *Nano Lett.*, 2014, **14**, 839-846.
28. Z. Zhang, Y. Liu, Y. Yang and B. I. Yakobson, *Nano Lett.*, 2016, **16**, 1398-1403.
29. J.-H. Park, J. C. Park, S. J. Yun, H. Kim, D. H. Luong, S. M. Kim, S. H. Choi, W. Yang, J. Kong, K. K. Kim and Y. H. Lee, *ACS Nano*, 2014, **8**, 8520-8528.
30. Y.-H. Lee, K.-K. Liu, A.-Y. Lu, C.-Y. Wu, C.-T. Lin, W. Zhang, C.-Y. Su, C.-L. Hsu, T.-W. Lin, K.-H. Wei, Y. Shi and L.-J. Li, *RSC Adv.*, 2012, **2**, 111-115.
31. H. Oh, J. Jo, Y. Tchoe, H. Yoon, H. H. Lee, S.-S. Kim, M. Kim, B.-H. Sohn and G.-C. Yi, *NPG Asia Mater.*, 2016, **8**, e330.
32. S. M. Kim, A. Hsu, M. H. Park, S. H. Chae, S. J. Yun, J. S. Lee, D.-H. Cho, W. Fang, C. Lee, T. Palacios, M. Dresselhaus, K. K. Kim, Y. H. Lee and J. Kong, *Nat. Commun.*, 2015, **6**, 8662.
33. S. Caneva, R. S. Weatherup, B. C. Bayer, B. Brennan, S. J. Spencer, K. Mingard, A. Cabrero-Vilatela, C. Baehtz, A. J. Pollard and S. Hofmann, *Nano Lett.*, 2015, **15**, 1867-1875.
34. T. Wu, X. Zhang, Q. Yuan, J. Xue, G. Lu, Z. Liu, H. Wang, H. Wang, F. Ding, Q. Yu, X. Xie and M. Jiang, *Nat. Mater.*, 2016, **15**, 43-47.
35. R. Y. Tay, S. H. Tsang, M. Loeblein, W. L. Chow, G. C. Loh, J. W. Toh, S. L. Ang and E. H. T. Teo, *Appl. Phys. Lett.*, 2015, **106**, 101901.
36. J. Chen, Y. Wen, Y. Guo, B. Wu, L. Huang, Y. Xue, D. Geng, D. Wang, G. Yu and Y. Liu, *J. Am. Chem. Soc.*, 2011, **133**, 17548-17551.
37. M. Wang, S. K. Jang, W.-J. Jang, M. Kim, S.-Y. Park, S.-W. Kim, S.-J. Kahng, J.-Y. Choi, R. S. Ruoff, Y. J. Song and S. Lee, *Adv. Mater.*, 2013, **25**, 2746-2752.
38. T. Gao, X. Song, H. Du, Y. Nie, Y. Chen, Q. Ji, J. Sun, Y. Yang, Y. Zhang and Z. Liu, *Nat. Commun.*, 2015, **6**, 6835.
39. X. Song, T. Gao, Y. Nie, J. Zhuang, J. Sun, D. Ma, J. Shi, Y. Lin, F. Ding, Y. Zhang and Z. Liu, *Nano Lett.*, 2016, **16**, 6109-6116.
40. Q. Li, Z. Zhao, B. Yan, X. Song, Z. Zhang, J. Li, X. Wu, Z. Bian, X. Zou, Y. Zhang and Z. Liu, *Adv. Mater.*, 2017, **29**, 1701325.
41. X. Ling, Y.-H. Lee, Y. Lin, W. Fang, L. Yu, M. S. Dresselhaus and J. Kong, *Nano Lett.*, 2014, **14**, 464-472.
42. M. Okada, T. Sawazaki, K. Watanabe, T. Taniguch, H. Hibino, H. Shinohara and R. Kitaura, *ACS Nano*, 2014, **8**, 8273-8277.
43. M. Zhang, Y. Zhu, X. Wang, Q. Feng, S. Qiao, W. Wen, Y. Chen, M. Cui, J. Zhang, C. Cai and L. Xie, *J. Am. Chem. Soc.*, 2015, **137**, 7051-7054.
44. S. Wang, X. Wang and J. H. Warner, *ACS Nano*, 2015, **9**, 5246-5254.
45. Z. Zhang, X. Ji, J. Shi, X. Zhou, S. Zhang, Y. Hou, Y. Qi, Q. Fang, Q. Ji, Y. Zhang, M. Hong, P. Yang, X. Liu, Q. Zhang, L. Liao, C. Jin, Z. Liu and Y. Zhang, *ACS Nano*, 2017, **11**, 4328-4336.
46. L. Fu, Y. Sun, N. Wu, R. G. Mendes, L. Chen, Z. Xu, T. Zhang, M. H. Ruemmeli, B. Rellinghaus, D. Pohl, L. Zhuang and L. Fu, *ACS Nano*, 2016, **10**, 2063-2070.
47. L. Niu, X. Liu, C. Cong, C. Wu, D. Wu, T. R. Chang, H. Wang, Q. Zeng, J. Zhou, X. Wang, W. Fu, P. Yu, Q. Fu, S. Najmaei, Z. Zhang, B. I. Yakobson, B. K. Tay, W. Zhou, H. T. Jeng, H. Lin, T. C. Sum, C. Jin, H. He, T. Yu and Z. Liu, *Adv. Mater.*, 2015, **27**, 7800-7808.
48. Z. Liu, Y. Gong, W. Zhou, L. Ma, J. Yu, J. C. Idrobo, J. Jung, A. H. MacDonald, R. Vajtai, J. Lou and P. M. Ajayan, *Nat. Commun.*, 2013, **4**, 2541.
49. K. Qian, R. Y. Tay, N. Viet Cuong, J. Wang, G. Cai, T. Chen, E. H. T. Teo and P. S. Lee, *Adv. Funct. Mater.*, 2016, **26**, 2176-2184.
50. J.-H. Meng, X. Liu, X.-W. Zhang, Y. Zhang, H.-L. Wang, Z.-G. Yin, Y.-Z. Zhang, H. Liu, J.-B. You and H. Yan, *Nano Energy*, 2016, **28**, 44-50.

TOC entry

A tutorial review of the state-of-the-art in the tailored growth of two-dimensional h-BN by virtue of CVD routes